

# Development of a soil electrical conductivity measurement system in paddy fields

The-Anh Ho<sup>1,2</sup>, Van-Huu Bui<sup>2</sup>, Van-Khanh Nguyen<sup>2</sup>, Dinh-Tu Nguyen<sup>1</sup>, Chi-Ngon Nguyen<sup>2</sup>

<sup>1</sup>Faculty of Mechanical Engineering, Can Tho University of Technology, Can Tho City, Vietnam

<sup>2</sup>Faculty of Automation, College of Engineering, Can Tho University, Can Tho City, Vietnam

## Article Info

### Article history:

Received Nov 7, 2023

Revised Feb 26, 2024

Accepted Mar 7, 2024

### Keywords:

Artificial neural network

Fixed electrode

Precision agriculture

Soil EC sensor Veris 3100

Soil electrical conductivity

Wenner method

## ABSTRACT

This study aims to develop a data collection system for measuring soil electrical conductivity (EC) in Paddy Fields using the Wenner measurement principle, with one electrode configuration based on the Veris 3100 measuring machine, and a second electrode configuration with fixed electrodes. The result is a system that measures soil EC using the fixed electrode configuration for more stable results compared to the coulter electrode configuration on the Veris 3100. This system comprises three main components: a 7-inch industrial touchscreen monitor used for real-time monitoring and storing collected data on external memory, a controller that provides reverse direct current (DC) power supply to the electrodes and measures voltage and current parameters on the electrodes, two mechanical configurations including six electrodes in contact with the soil. The system is developed to operate best after soil preparation and before seed sowing. The collected data is processed and compared to actual measurements using an artificial neural network (ANN), resulting in an  $R^2=0.7449$ , equivalent to linear regression. The system has been successfully installed and operated on a handheld tractor and tested in Paddy Fields on the outskirts of Can Tho City, Vietnam.

*This is an open access article under the [CC BY-SA](https://creativecommons.org/licenses/by-sa/4.0/) license.*



## Corresponding Author:

Chi-Ngon Nguyen

Faculty of Automation, College of Engineering, Can Tho University

Campus II, 3/2 Street, Xuan Khanh Ward, Can Tho City, Vietnam

Email: nngon@ctu.edu.vn

## 1. INTRODUCTION

Rice is considered the most important staple crop in many Asian countries, playing a crucial role in ensuring food security and exports in countries like Vietnam [1]. In the Vietnam Mekong Delta (VMD) region, which is known for its vast floodplains, a significant portion of agricultural land is dedicated to rice cultivation, contributing to approximately 85% of the annual rice export volume. However, these agricultural lands are often fragmented, vulnerable, and heavily impacted by climate change and saline intrusion [2]–[6]. The adoption of modern technologies in rice production is still in its infancy, with most farming practices relying on traditional methods and individual experiences based on recommendations from agricultural extension services or farming cooperatives [7]. Studies on the use of soil electrical conductivity (EC) indices in this area have been conducted [8]–[13]. However, most of these studies utilize laboratory-based analysis methods and the lack of instruments can measure EC automatically in this area.

Soil EC is an index of soil salinity and specific soil properties, it serves as a tool for monitoring fertilizer in precision agriculture [14]–[19]. In a survey of studies conducted by Corwin [20] in 2019 on the apparent electrical conductivity of soil (ECa) based on 470 relevant documents, various soil properties were directly measured in the field, including salinity-encompassing total dissolved solids, dissolved solids,

inorganic carbon (C), calcium carbonate ( $\text{CaCO}_3$ ), and nutrients (237 studies); water content-including macropore porosity, groundwater depth, and irrigation channel permeability (105 studies); structural attributes-including sand, clay, depth to clay or sand layer, soil layer, soil surface depth, depth to bedrock, saturation ratio, soil type, and mapping units (133 studies). Soil EC is not always directly related to crop yield, however, mapping Soil EC can explain yield variations at different locations in the field [21]. Additionally, due to the impacts of global climate change and rising sea levels on agriculture worldwide, as recommended by the Soil Science Society of America. The agricultural land in the VMD region is currently severely affected by saline intrusion. Soil EC is also used as an effective tool for managing soil salinity in agricultural lands [15], [22]–[27].

Most studies using the Veris 3100 system [28], [29] have been effectively conducted in arid and semi-arid regions on wheat, maize, and soybean crops. Some studies have been carried out in rice fields during the post-harvest and pre-tillage stages [30], [31]. The Veris 3100 system [32], comprising six coulters, is used to map EC according to two coulters configurations. Its technical specifications are presented in Table 1. The center coulters, spaced approximately 30 cm apart, are used to measure soil resistance at depths of 0-30 cm, while the outer coulters, spaced approximately 90 cm apart, are used to measure resistance at depths of 0-90 cm. A prerequisite for the system to operate effectively is that the coulters must be submerged approximately 6 cm deep in stable soil [30], [33]. Due to its significant weight, there is currently no evidence of this system operating effectively on the soft soils of rice fields. So, there is a need for a suitable soil EC measurement system that can be effective in soft soil conditions for rice cultivation in the VMD region.

Table 1. The configuration of the Veris 3100 system

Features of soil sensor	Specification
Overall dimensions: implement	Width: 92.5" (235 cm); Length: 96" (244 cm); Height: 35" (89 cm)
Weight: basic implement without weight package	1200 lbs (544 kg)
Minimum horsepower required:	30 hp (requirements will vary based on speed, terrain, and soil conditions)
Coulter-electrode blade diameter:	17" (43 cm); thickness 4mm; with tapered roller bearings and cast-iron hubs
Max. field speed	15 mph (25 km/h)
2" ball coupler and safety chain	7,000 lb. rating (3173 kg)
Maximum road speed	55 mph (25 km/h)

Today, artificial neural networks (ANN) have been widely used in various fields. ANN demonstrates superior effectiveness compared to traditional methods when calibrating nonlinear systems [34]. A study conducted at A Central University-New Delhi calibrated a temperature sensor negative temperature coefficient using an ANN, achieving an accuracy after calibration of 95% [35]. In a study at Carnegie Mellon University-USA, an ANN was used to calibrate low-cost air sensors ( $\text{CO}$ ,  $\text{NO}_2$ ,  $\text{CO}_2$ , and  $\text{O}_3$ ), yielding calibration results with relative errors of approximately 14% for  $\text{CO}$ , 2% for  $\text{CO}_2$ , 29% for  $\text{NO}_2$ , and 15% for  $\text{O}_3$  [36].

The study aims to develop a tool for collecting soil EC data under rice cultivation conditions in the VMD. The soil layer at depths of 0-20 cm significantly impacts rice growth and development, with rice roots concentrated at depths of 0-10 cm. Therefore, the system needs to collect data in this soil layer for further research. The soil EC parameters are referenced with global positioning system (GPS) data to enable the system to operate in different areas. ANN is proposed to calibrate the values obtained from the fixed electrodes configuration and the HI88331 Hanna soil EC meter in nonlinear conditions due to soil heterogeneity, providing a solution for further research on rice crops when combined with other soil indices.

## 2. MATERIAL AND METHODS

### 2.1. Development of structure

#### 2.1.1. Principles of resistivity measurement

The four-electrode method discovered by Wenner [37] is still used in electrical resistivity surveys in the field of geophysics today. The method involves placing the electrodes a distance ( $a$ ) apart and passing a current through two electrodes ( $A$ ,  $B$ ) while measuring the voltage drop across two different electrodes ( $M$ ,  $N$ ). The voltage difference  $\Delta U_1(V)$  is calculated from this measurement (Figure 1). At the same time, the voltage drop is measured at electrodes ( $K$ ,  $H$ ) to calculate  $\Delta U_2(V)$ .

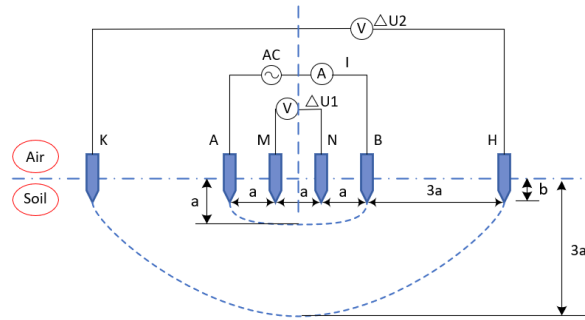


Figure 1. Theoretical representation of the electrical resistance measurement

Soil can be considered as a resistor, and in that case, the formula for soil resistance is calculated using (1).

$$R(\Omega) = \frac{\Delta U}{I} \quad (1)$$

Where  $I(A)$  is the current supplied into the soil at electrodes (A, B),  $\Delta U_1 (V)$  is the potential difference measured at points (M, N) to calculate the resistance at a depth of  $a (m)$ ,  $\Delta U_2 (V)$  is the potential difference measured at points (K, H) to calculate the resistance at a depth of  $3a (m)$  (Figure 1).

Soil resistivity is the resistance calculated per unit length between the two electrodes when the electrode diameter is less than 10 times the distance. The soil resistivity is calculated using (2) [37].

$$\rho(\Omega \cdot m) = \frac{4\pi a R}{I + \frac{2a}{\sqrt{a^2 + b^2}} - \frac{2a}{\sqrt{a^2 + b^2}}} = 2\pi a \frac{\Delta U(V)}{I(A)} \quad (2)$$

Or:

$$\rho(\Omega \cdot m) = 2\pi a R \quad (3)$$

$$\text{When the distance } b \text{ is greater than } a, \text{ we have the formula: } \rho(\Omega \cdot m) = 4\pi a R \quad (4)$$

$$\text{When the distance } b \text{ is smaller than } a, \text{ we have the formula: } \rho(\Omega \cdot m) = 2\pi a R \quad (5)$$

### 2.1.2. Mechanical fabrication

Land preparation is the initial stage that plays a crucial role in rice cultivation; the rice yield in fields that are prepared is higher compared to those that are not [38]. The optimal depth for land preparation is typically around 17 to 20 cm, which is considered ideal and recommended for farmers. Working the soil at this depth improves productivity and reduces rice lodging [39], [40]. The majority of the rice root mass is concentrated within the 0 to 10 cm depth range, with root density decreasing significantly at greater depths [41]. However, the non-uniform soil structure in fields leads to varied rice growth patterns based on the spatial distribution of the area [42].

#### i) Electrode configuration based on the Veris 3100 device

The mechanical part consists of 6 metal discs with a diameter of  $40 \times 0.3$  cm, which are interconnected and insulated from the main rod through a shock-absorbing joint. The shock-absorbing joint helps to withstand strong impacts between the ground and the mechanical system. Additionally, with this mechanism, the discs have better contact with the ground when moving on uneven surfaces. Coulters 2 and 5 are used for injecting electrical current into the soil. Coulters 1 and 6 are used to measure soil EC at a depth of 45 cm (expandable up to 90 cm), while Coulters 3 and 4 are used to measure EC at a shallow depth of 15 cm (expandable up to 30 cm). The main rod is combined with a triangular iron frame that can be connected to different tractors at the connecting joint. There are tall supporting posts on the iron frame for installing GPS antennas. The overall dimensions of the system are length 135 cm, width 155 cm, height 67 cm (excluding the GPS antenna), and it weighs 76 kg (Figure 2). At each coulter-electrode, additional Polyvinyl Chloride (PVC) plastic plates are installed to limit the depth of the coulter-electrodes when they come into contact with the ground. These plastic plates will prevent the coulter electrodes from sinking too deeply when moving on soft ground.

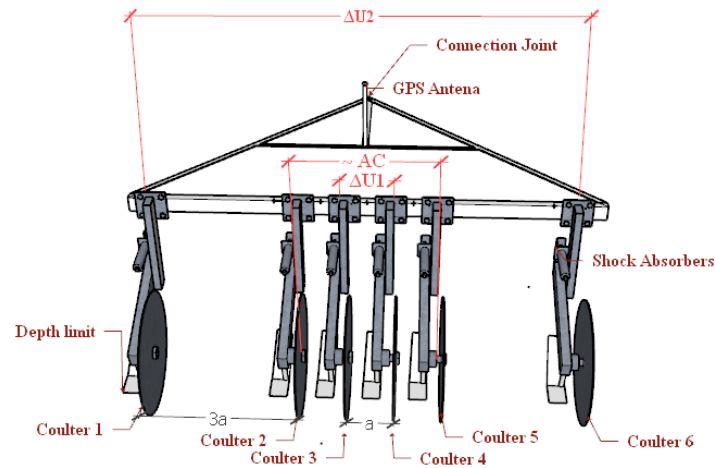


Figure 2. Design electrode system using coulter

ii) The fixed electrode configuration

The mechanical part consists of 6 semi-cylindrical electrodes with a height of 8 cm (circular discs of 30 cm diameter) mounted on a wooden board measuring 400×1200 mm, with the electrode spacing adjustable as desired. The electrodes are fixed in height on the wooden board, which serves both as the EC sensor and a device that can be used to flatten the field surface during soil preparation. An insulating layer is applied to ensure that only the two metal faces of the electrodes come into contact with the soil during operation, reducing interference for the sensor to operate in wet soil conditions (Figure 3).



Figure 3. The fixed electrodes when mounted on the wooden board

### 2.1.3. Data acquisition

The block diagram of the data acquisition system functions by supplying power to the coulter and collecting voltage values at the remaining coulter. The GPS coordinates and conductivity data are calculated on the controller, and the human-machine interface (HMI) display receives values from the controller and stores them in external memory. There are two data storage options, including automatic sampling with a sampling interval of 1 second and manual sampling when operating the button on the HMI. The entire system is powered by a 12 V battery (Figure 4).

### 2.1.4. The global positioning system data acquisition system

The GPS receiver module supports RS-485 communication and has the following specifications: power supply +5 to +30 V, current consumption of 100 mA, 56-channel receiver, manufacturer's accuracy of 2.5 m, reverse polarity protection, dimensions of 117×72×35 mm, and operating temperature range from -40 to +85 °C. During actual operation, the coordinate update takes up to 5 seconds. Therefore, after collecting GPS data, it is formatted in the National Marine Electronics Association (NMEA) and then converted to coordinate format (x, y). The vehicle moves in a rectangular shape in the rice field, but samples are only taken in the forward direction with a sampling rate of 1 second. For point-to-point measurement, an average of about 3 data samples is taken, with a measurement time at each point ranging from 5 to 10 seconds to ensure that the GPS coordinates are updated.

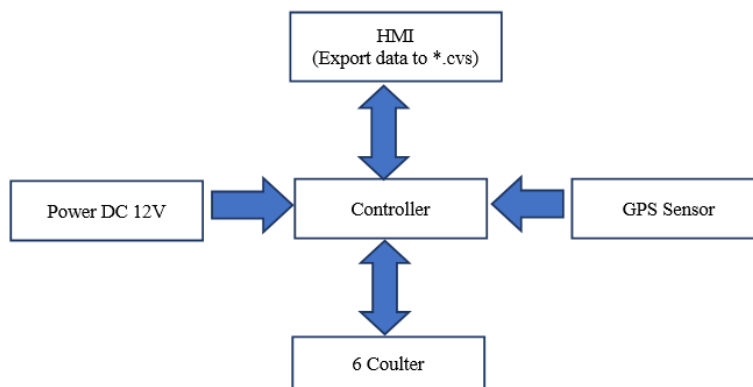


Figure 4. The block diagram of the data acquisition

### 2.1.5. Calibration

Before using the tractor for field measurements, the coulter-electrodes are calibrated in water. Due to the salinity of the water in the field, which is influenced by seawater containing NaCl, salt is used in this calibration process to match real-life conditions. Quantitative salt in small bags 2 g by Ohaus bench scale (USA) with error 10 mg. Because the fixed electrodes are partially cut from circular disks, this calibration step is not performed.

The Hanna HI98331 conductivity meter, which has a measurement range of 0 to 4 mS/cm, has been calibrated using the recommended standard solution from the manufacturer. It has then been compared to the results obtained using the coulter-electrodes system in a homogeneous water environment, with salt being used to vary the conductivity of the solution. The coulter-electrodes are fixed on a horizontal axis and can be adjusted to the desired height. After each change in the conductivity of the solution, the EC values at depths of 2.5, 6.5, 10.5, and 14.5 cm of the coulter-electrodes are recorded (Figure 5).



Figure 5. Measuring EC in water

## 2.2. Experimental setup

The experiment was arranged in the field on an area of 1.4 ha at latitude 10°01'27.2"N, longitude 105°34'45.1"E, and another area 0.4 ha at latitude 10°01'35.4"N, 105°37'11.6"E in Thoi Lai district of Can Tho city, Vietnam. For the coulter configuration, four coulter electrodes with a spacing of 15 cm between electrodes (minimum spacing), along with four fixed electrodes with a spacing of 10 cm between electrodes are used. Initially, the coulter electrodes are pulled across the field in a predetermined straight line at a speed of approximately 3 km/h, continuously sampling at a rate of 1 s intervals. The experiment is repeated with the coulter electrodes replaced by fixed electrodes. Afterward, the fixed points were measured using Hanna equipment, and the data collected from the fixed electrodes were reprocessed. The results of this process were calibrated using ANN.

### 2.3. Structure of artificial neural network

In this study, the ANN toolbox integrated into the MATLAB R2017 software was used to calibrate the measurement results. The measurements from the Hanna HI98331 device were considered as the reference values. The ANN consists of three main components (Figure 6); i) Input layer: provides the necessary data to the network. The number of neurons in the input layer corresponds to the number of input parameters provided to the network, and these input parameters are assumed to be in vector form; ii) Hidden layer: contains hidden neurons that connect input values to output values. A neural network can have one or multiple hidden layers that are primarily responsible for processing the neurons in the input layer and passing information to the neurons in the output layer. These neurons adapt to the classification and recognition of the relationship between input and output parameters; and iii) output layer: contains output neurons that transfer the output information from the ANN to the user. An ANN can be constructed to have multiple output parameters.

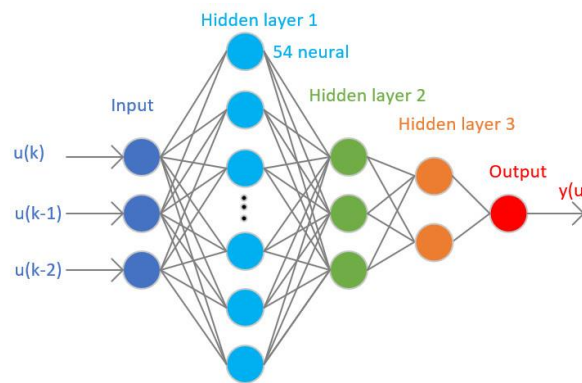


Figure 6. Structure of ANN

In this study, the following basic parameters were used in the neural network (NN) toolbox: the Levenberg-Marquardt algorithm was used for training and testing the data. The mathematical model of the ANN propagates straight [43], [44].

$$y(u) = f(\sum_{i=1}^n w_i u_i) \quad (6)$$

Where:

$y(u)$ : output value according to variable  $u(k)$

$f$ : trigger function

$w_i$ : the binding weight of the neural

$u_i$ : input value

The network training process is the essence of an ANN operation management, multilayer networking, and reverse propagation training used in the MATLAB toolbox works as follows:

Step 1: the input parameter is entered into the neural in the input layer.

$$a^0 = u \quad (7)$$

Step 2: at the  $i^{\text{th}}$  hidden layer neural.

$$z_{inj} = b_{0j} + \sum_{i=1}^n u_i v_{ij} \quad (8)$$

Step 3: the trigger function will be used to convert the received value into an output value.

$$z_j = f(z_{inj}) \quad (9)$$

Next, the output value of the latent layer neural  $j$  is transmitted to the next layer neural similar to the method from the input layer to the hidden layer.

$$y_{ink} = w_{0k} + \sum_{i=1}^p z_j w_{ik} \quad (10)$$

The trigger function is further used to calculate the output value at the next neural. The end of this stage will move to the process of reverse propagation.

Step 4: in the input class, each input subset value is accompanied by the actual value and calculates the corresponding error value (activation function – J).

$$J = t_k - y_k \quad (11)$$

Step 5: the derivative of the activation function J is just found according to the weight between the hidden class, the output class, and the weight of the input class, the hidden class.

$$\Delta w_{jk} = \frac{\partial J}{\partial w_{jk}} \quad (12)$$

$$\Delta v_{ij} = \frac{\partial J}{\partial v_{ij}} \quad (13)$$

Step 6: continues, the link weighting is updated again.

$$w_{jk}(new) = w_{jk}(old) + \alpha \Delta w_{jk} \quad (14)$$

$$v_{ij}(new) = v_{ij}(old) + \alpha \Delta v_{ij} \quad (15)$$

After collecting field data, the two fields were divided into two main subsets: i) Subset 1 (training data) consisted of 232 pairs of EC measurement values from the fixed electrodes and Hana device. Among these, 70% of the data, corresponding to 162 input samples, was used to train the network. Cross-validation accounted for 15% of the data, corresponding to 35 input sample sets, and was used to check for overfitting. Network testing accounted for the remaining 15% of the data, corresponding to 35 input sample sets, and was used to assess the network's effectiveness during and after training; ii) Subset 2 (testing data) consisted of 117 input sample values and 117 corresponding EC measurement values from the Hanna device. It aimed to assess the reliability of the newly trained network and enable the prediction of EC values for different locations.

Overfitting refers to when a model becomes too tightly fit to the training data, which can result in significant consequences if there is noise present in the training dataset. It means that the model does not generalize well to data outside the training set. Overfitting especially occurs when the training data is small or when the model is overly complex.

Validation is a technique where a small subset is taken from the training data set, and the model is evaluated on this subset. This subset is referred to as the validation set, while the remaining part of the original training set becomes the new training set for the model. The results of the network training process show the mean squared error (MSE) and correlation coefficient (R) for three subsets derived from subset 1, which are the training data set error, cross-validation error, and network testing error.

After the training process, the 117 input sample values in subset 2 are tested and compared with the corresponding 117 measured values. The R-squared coefficient is used to evaluate the estimation results from the model and the measured values from the actual device in Excel software. The linear regression equation from subset 1 will be established as a basis for comparison with the estimated results from the ANN.

### 3. RESULTS AND DISCUSSION

#### 3.1. Mechanical system and operation

After being manufactured, the mechanical system is connected to a Yanmar 494 tractor and operated before plowing. Figure 7 shows the system in the field prior to and during land preparation. In paddy fields after harvesting, there is a minimum of 20 cm or more of remaining rice stubble [45], combined with dry and hard soil, therefore, the coulter-electrodes cannot make contact with the soil (Figure 7(a)). In this case, neither of the two electrode configurations can conduct measurements.

The soil becomes softer after water is introduced into the field for 1 to 2 days and plowing is carried out, followed by drainage before seed sowing. A hand tractor is used during the land preparation phase (Figure 7(b)), and the measurement is performed immediately after field drainage and before seed sowing (Figure 7(c)). The depth of the coulter electrodes is kept stable at certain positions thanks to limiting plastic plates; however, in waterlogged areas, these plates no longer limit the depth effectively, resulting in significantly large measurement errors. Fixed electrodes become highly efficient for measurements in this environment (Figure 8).

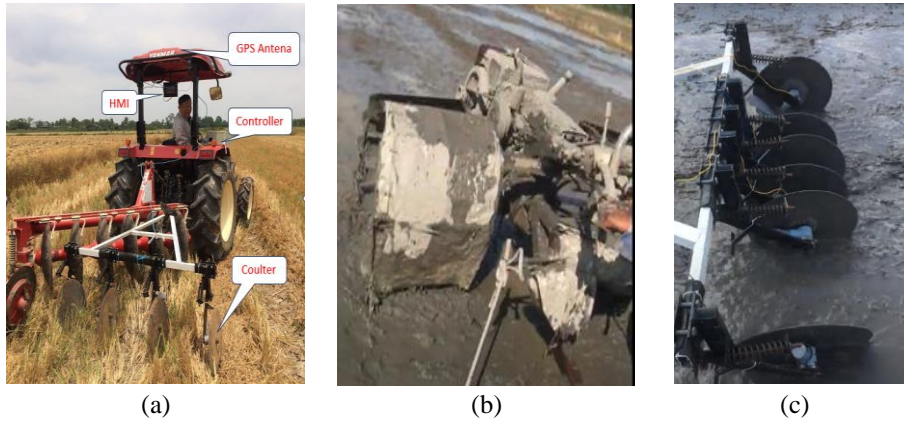


Figure 7. Operating the system in the field prior to and during land preparation (a) installed in tractor Yanmar-494, (b) hand tractor for a small farm, and (c) structure of soil EC sensor

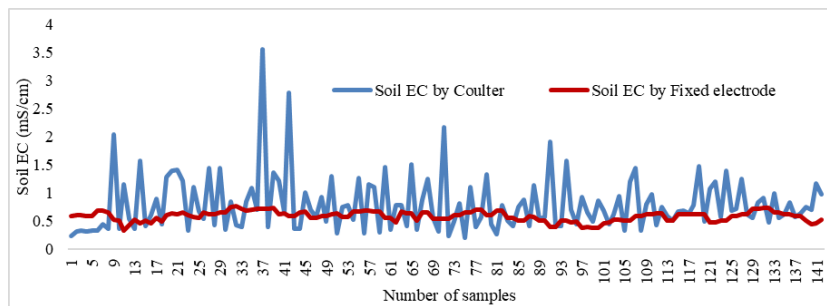


Figure 8. Soil EC results from two methods

**3.2. Calibration results in a water environment**

Fresh water was contained in a 120-litre cylindrical plastic tank. Salt was added to adjust the EC value of the water. The salinity of saltwater increases by 16.7 ppm, corresponding to its EC increasing by 0.047 mS/cm. The obtained results show that when using measurement discs with good linearity and correlation with values obtained from the Hanna device. Especially, with an electrode distance of 10 cm combined with an electrode depth adjustment of 10.5 cm, a high EC value is obtained, equivalent to twice the value obtained from the Hanna device (Figure 9). This result is consistent with previously published results using the Wenner [37] measurement method and serves as the basis for establishing the depth limit for measurements in the soil environment.

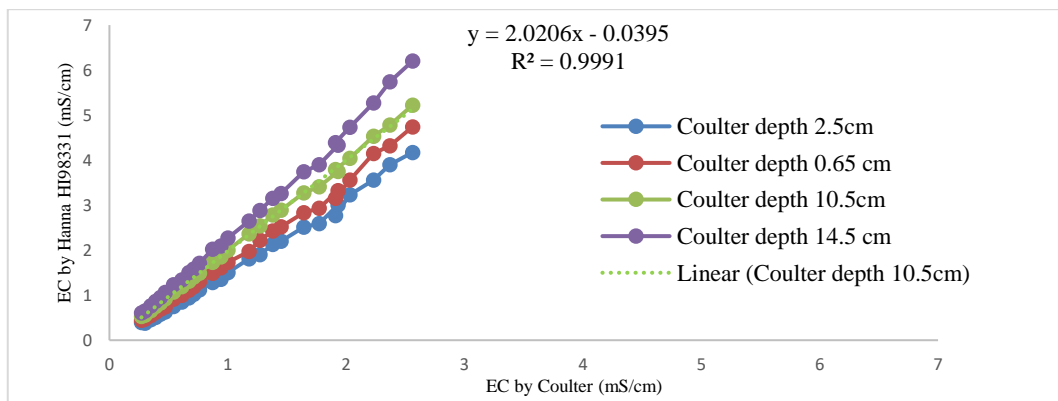


Figure 9. The influence of electrode depth on measurement results



### 3.3. Data acquisition and processing results

The data acquisition time with a sampling cycle of 1 second and a distance of 700 m took a total of 15 minutes with 837 data sampling points. Meanwhile, the Veris system collected data with approximately 1,800 points in 30 [46]. The training process was performed by using a first hidden layer and gradually increasing the number of neurons until the output error value was acceptable but not exceeding 100. Then, the number of neurons in the next layer was increased. This process was repeated and the result with the best error value according to the desired outcome was selected. The training process stopped when the validation error increased within six iterations, occurring at the 14<sup>th</sup> iteration. There were no significant errors at epoch 8, where the best validation performance occurred. The results showed that the MSE=0.0031715 (Figure 10).

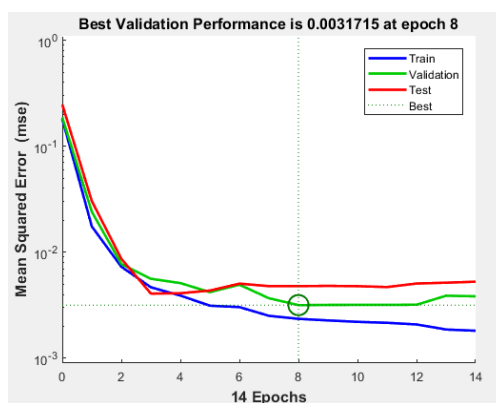


Figure 10. Training results of the ANN

Output tracking of targets is very good for training, testing, and validation, with an  $R=0.9318$  for overall response (Figure 11). After passing the input values through the ANN network, the results have a good correlation with the data collected from real life,  $R^2 = 0.7449$ . The estimated results obtained after inputting 117 values from subset 2 into the linear regression equation derived from subset 1 are equivalent to the estimated values from the ANN. This indicates that using the soil conductivity measurement system with fixed electrodes is highly reliable and can be applied for further research in the future.

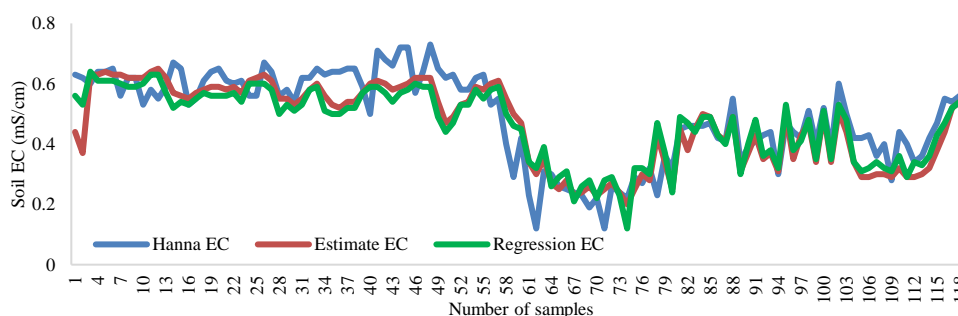


Figure 11. The results of comparing estimated data after training, regression equations, and measurement values from the Hanna device

### 3.3. Discussion

Measuring soil EC using the fixed electrode method in soft soil environments has yielded quite impressive results. This measurement approach can be utilized for further studies on soil properties. However, the timeframe for conducting measurements is very short, from land preparation to seed sowing, necessitating specific seasonal plans for broader implementation. Although the coulter electrode method for measuring soil EC is limited in soft soil environments, it has proven to be effective in numerous studies in dry soil conditions. Therefore, further research is needed in different soil conditions to obtain a more comprehensive understanding.

Although the system has been calibrated and tested successfully with good results in rice cultivation fields, the Hanna measuring device is limited to a range of 0 to 4 mS/cm, so it cannot be used to test

environments with higher water EC. During the operation of the system, the authors did not have much data on soil properties in the area, so further research is needed on the correlation between soil EC and other indicators. During operation, the GPS data collection device has an update time of about 5 seconds, which can cause difficulties in data processing when operating in larger areas. Soil EC measurements referenced with GPS coordinates will be used for mapping in future studies. When the correlation between the measured value and the benchmark value does not follow a simple mathematical function, the use of ANN with a learning mechanism, allows this nonlinear relationship to be determined.

#### 4. CONCLUSION

Through field experiments measuring soil EC in rice cultivation conditions in the VMD region, two electrode configurations, a coulter electrode, and fixed electrodes, were tested. The system performed best when using the fixed electrode configuration. To achieve optimal results with the Wenner electrode configuration, it is crucial to standardize the depth of penetration for both configurations. In dry soil conditions, depth is controlled through fixed-depth tillage, conversely, in wet soil conditions, the heterogeneous soil structure is more pronounced, requiring precise depth control for the electrodes' penetration into the soil to obtain better measurement results.

Mapping soil EC has been proven to not only be used for monitoring soil salinity in agricultural land but also as an effective tool for precision farming. The data acquisition system has been connected and operated with tractors in rice fields. The best time to operate in the rice fields is during the post-tillage and pre-seeding stages because the soil is softer, ensuring good contact between the electrode and the soil without data loss. The field collection process provided information on soil EC in the rice fields, with 837 points collected in about 15 minutes. The estimated soil EC results after training through a neural network obtain the  $R^2=0.7449$ . With this method, further research can be conducted on the physical properties, chemical properties, and salinity of soil under rice cultivation conditions in the VMD region. Studies on measuring soil salinity and soil properties spatially across the field will be conducted in future studies




#### REFERENCES

- [1] K. Clauss, M. Ottinger, P. Leinenkugel, and C. Kuenzer, "Estimating rice production in the Mekong Delta, Vietnam, utilizing time series of sentinel-1 sar data," *International Journal of Applied Earth Observation and Geoinformation*, vol. 73, pp. 574–585, 2018, doi: 10.1016/j.jag.2018.07.022.
- [2] L. C. B. Tho and C. Umetsu, "Sustainable farming techniques and farm size for rice smallholders in the Vietnamese Mekong Delta: a slack-based technical efficiency approach," *Agriculture, Ecosystems, and Environment*, vol. 326, 2022, doi: 10.1016/j.agee.2021.107775.
- [3] D. D. Tran and J. Weger, "Barriers to implementing irrigation and drainage policies in an Giang Province, Mekong Delta, Vietnam," *Irrigation and Drainage*, vol. 67, pp. 81–95, 2018, doi: 10.1002/ird.2172.
- [4] T. Q. Toan, "Climate change and sea level rise in the Mekong Delta: flood, tidal inundation, salinity intrusion, and irrigation adaptation methods," *Coastal Disasters and Climate Change in Vietnam: Engineering and Planning Perspectives*, pp. 199–218, 2014, doi: 10.1016/B978-0-12-800007-6.00009-5.
- [5] L. T. T. Dang, A. H. Tran, T. L. T. Vu, and T. A. T. Nguyen, "Assessment of the impact of climate change and cultivation conditions on rice yield in Vietnamese Mekong Delta. a case study in Vinh Thanh District, Can Tho City," *IOP Conference Series: Earth and Environmental Science*, vol. 1170, no. 1, 2023, doi: 10.1088/1755-1315/1170/1/012001.
- [6] N. Q. L. Tran, D. Connell, T. H. Nguyen, and D. Phung, "Climate change and water-related diseases in the Mekong Delta Region," *Oxford Research Encyclopedia of Global Public Health*, 2023, doi: 10.1093/acrefore/9780190632366.013.460.
- [7] D. M. Ngo, H. S. Doan, and V. T. Mai, "A review of precision agriculture in rice production in Vietnam," *FFTC Agricultural Policy Platform (FFTC-AP)*, 2019, [Online]. Available: <https://ap.ffc.org.tw/article/1418>
- [8] L. V. Tan, T. Tran, and H. H. Loc, "Soil and water quality indicators of diversified farming systems in a saline region of the Mekong Delta, Vietnam," *Agriculture (Switzerland)*, vol. 10, no. 2, 2020, doi: 10.3390/agriculture10020038.
- [9] K. A. Nguyen, Y. A. Liou, H. P. Tran, P. P. Hoang, and T. H. Nguyen, "Soil salinity assessment by using near-infrared channel and vegetation soil salinity index derived from landsat 8 oli data: a case study in the Tra Vinh Province, Mekong Delta, Vietnam," *Progress in Earth and Planetary Science*, vol. 7, no. 1, 2020, doi: 10.1186/s40645-019-0311-0.
- [10] V. H. Nguyen, J. Germer, V. N. Duong, and F. Asch, "Soil resistivity measurements to evaluate subsoil salinity in rice production systems in the Vietnam Mekong Delta," *Near Surface Geophysics*, vol. 21, no. 4, pp. 288–299, 2023, doi: 10.1002/nsg.12260.
- [11] L. V. Tan and T. Thanh, "The effects of salinity on changes in characteristics of soils collected in a saline region of the Mekong Delta, Vietnam," *Open Chemistry*, vol. 19, no. 1, pp. 471–480, 2021, doi: 10.1515/chem-2021-0037.
- [12] V. H. Nguyen, J. Germer, and F. Asch, "Evaluating topsoil salinity via geophysical methods in rice production systems in the Vietnam Mekong Delta," *Journal of Agronomy and Crop Science*, vol. 210, no. 1, 2024, doi: 10.1111/jac.12676.
- [13] T. V. Tran *et al.*, "Examining spatiotemporal salinity dynamics in the Mekong River Delta using landsat time series imagery and a spatial regression approach," *Science of the Total Environment*, vol. 687, pp. 1087–1097, 2019, doi: 10.1016/j.scitotenv.2019.06.056.
- [14] E. Lück, R. Gebbers, J. Ruehlmann, and U. Spangenberg, "Electrical conductivity mapping for precision farming," *Near Surface Geophysics*, vol. 7, no. 1, pp. 15–25, 2009, doi: 10.3997/1873-0604.2008031.
- [15] D. L. Corwin and E. Scudiero, "Field-scale apparent soil electrical conductivity," *Soil Science Society of America Journal*, vol. 84, no. 5, pp. 1405–1441, 2020, doi: 10.1002/saj2.20153.
- [16] S. P. Friedman, "Soil properties influencing apparent electrical conductivity: a review," *Computers and Electronics in*




- Agriculture*, vol. 46, no. 1-3 SPEC. ISS., pp. 45–70, 2005, doi: 10.1016/j.compag.2004.11.001.
- [17] B. Sahu, S. Chatterjee, S. Mukherjee, and C. Sharma, “Tools of precision agriculture: a review,” ~2692~ *International Journal of Chemical Studies*, vol. 7, no. 6, pp. 2692–2697, 2019.
- [18] C. Perry, G. Vellidis, K. Rucker, and D. Sullivan, “Using soil electrical conductivity to map nematode-prone areas in agricultural fields,” in *2006 ASAE Annual Meeting, Portland, Oregon, July 9-12, 2006*, St. Joseph, MI: American Society of Agricultural and Biological Engineers, 2006, doi: 10.13031/2013.20585.
- [19] J. M. Terrón, J. M. D. Silva, F. J. M. García, and D. Becerra, “Soil electric apparent conductivity as a decision supporting tool on fertilization,” in *15th World Fertilizer Congress of The International Scientific Centre For Fertilizers (CIEC)*, Bucharest, Romania, 2010, pp. 1–10, doi: 10.13140/RG.2.1.3913.1361.
- [20] D. Corwin, “Compilation of literature using apparent soil electrical conductivity with geophysical techniques to measure soil properties,” *Journal Korean Acad Fam Med*, vol. 20, no. 8, pp. 978–990, 2019.
- [21] R. Grisso, M. Alley, W. G. Wysor, D. Holshouser, and W. Thomason, “Precision farming tools: soil electrical conductivity,” *Precision Farming Tools: Soil Electrical Conductivity, Virginia Cooperative Extension Publication*, pp. 1–6, 2009.
- [22] D. L. Corwin, “Climate change impacts on soil salinity in agricultural areas,” *European Journal of Soil Science*, vol. 72, no. 2, pp. 842–862, 2021, doi: 10.1111/ejss.13010.
- [23] D. L. Corwin and R. E. Plant, “Applications of apparent soil electrical conductivity in precision agriculture,” *Computers and Electronics in Agriculture*, vol. 46, no. 1-3 SPEC. ISS., pp. 1–10, 2005, doi: 10.1016/j.compag.2004.10.004.
- [24] D. L. Corwin and K. Yemoto, “Salinity: electrical conductivity and total dissolved solids,” *Soil Science Society of America Journal*, vol. 84, no. 5, pp. 1442–1461, 2020, doi: 10.1002/saj.20154.
- [25] J. D. Rhoades and A. D. Halvorson, “Electrical conductivity methods for detecting and delineating saline seeps and measuring salinity in northern great plains soils,” *Ars-W*, p. 45, 1977.
- [26] J. D. Rhoades, “Electrical conductivity methods for measuring and mapping soil salinity,” *Advances in Agronomy*, vol. 49, no. C, pp. 201–251, 1993, doi: 10.1016/S0065-2113(08)60795-6.
- [27] J. D. Rhoades, “Salinity: electrical conductivity and total dissolved solids,” in *Methods of Soil Analysis. Part 3. Chemical Methods-SSSA*, 5th ed., U.S. Salinity Laboratory, Riverside, California: 677 S. Segoe Rd., Madison, 1996, pp. 417–435, doi: 10.2136/sssabookser5.3.c14.
- [28] I. M. Puiu, G. Morar, G. Olteanu, and M. Ianoși, “Potato crop monitoring using veris mobile sensor platform,” *Bulletin of University of Agricultural Sciences and Veterinary Medicine Cluj-Napoca. Agriculture*, vol. 70, no. 1, pp. 113–117, 2013, doi: 10.15835/buasvmcn-agr:9776.
- [29] A. Uribeetxebarria, J. Arnó, A. Escolà, and J. A. Martínez-Casasnovas, “Apparent electrical conductivity and multivariate analysis of soil properties to assess soil constraints in orchards affected by previous parcelling,” *Geoderma*, vol. 319, pp. 185–193, 2018, doi: 10.1016/j.geoderma.2018.01.008.
- [30] A. Gholizadeh, M. A. M. Soom, A. R. Anuar, and W. Aimrun, “Relationship between apparent electrical conductivity and soil physical properties in a Malaysian paddy field,” *Archives of Agronomy and Soil Science*, vol. 58, no. 2, pp. 155–168, 2012, doi: 10.1080/03650340.2010.509132.
- [31] R. P. A. Setiawan, Desrial, M. Solahudin, I. W. Astika, S. Widodo, and D. Danindra, “Veris 3100 application for determining the fertility of rice fields before land preparation,” *IOP Conference Series: Earth and Environmental Science*, vol. 1038, no. 1, 2022, doi: 10.1088/1755-1315/1038/1/012036.
- [32] M. A. Azmi, R. Mohammad, and D. E. Pebrian, “Evaluation of soil EC mapping driven by manual and autopilot-automated steering systems of tractor on oil palm plantation terrain,” *Food Research*, vol. 4, no. 5, pp. 62–69, 2020, doi: 10.26656/fr.2017.4(S5).015.
- [33] C. K. Johnson, J. W. Doran, H. R. Duke, B. J. Wienhold, K. M. Eskridge, and J. F. Shanahan, “Field-Scale electrical conductivity mapping for delineating soil condition,” *Soil Science Society of America Journal*, vol. 65, no. 6, pp. 1829–1837, 2001, doi: 10.2136/sssaj2001.1829.
- [34] A. M. M. Almassri, W. Z. W. Hasan, S. A. Ahmad, S. Shafie, C. Wada, and K. Horio, “Self-calibration algorithm for a pressure sensor with a real-time approach based on an artificial neural network,” *Sensors (Switzerland)*, vol. 18, no. 8, 2018, doi: 10.3390/s18082561.
- [35] S. A. Khan, T. Islam, and G. Husain, “Artificial neural network based online sensor calibration and compensation,” *International Journal of Computing*, vol. 6, no. 3, pp. 74–78, 2014, doi: 10.47839/ijc.6.3.454.
- [36] N. Zimmerman *et al.*, “A machine learning calibration model using random forests to improve sensor performance for lower-cost air quality monitoring,” *Atmospheric Measurement Techniques*, vol. 11, no. 1, pp. 291–313, 2018, doi: 10.5194/amt-11-291-2018.
- [37] F. Wenner, “A method of measuring earth resistivity,” *Bulletin of the Bureau of Standards*, vol. 12, no. 4, May 1916, doi: 10.6028/bulletin.282.
- [38] P. K. Sharma, S. K. D. Datta, and C. A. Redulla, “Tillage effects on soil physical properties and wetland rice yield,” *Agronomy Journal*, vol. 80, no. 1, pp. 34–39, 1988, doi: 10.2134/agronj1988.00021962008000010008x.
- [39] D. Gong, G. Dai, Y. Chen, and G. Yu, “Optimal tillage depths for enhancing rice yield, quality and lodging resistance in the rice production systems of Northeast China,” *PeerJ*, vol. 11, 2023, doi: 10.7717/peerj.15739.
- [40] T. B. Linh, S. Sleutel, G. V. Thi, K. L. Van, and W. M. Cornelis, “Deeper tillage and root growth in annual rice-upland cropping systems result in improved rice yield and economic profit relative to rice monoculture,” *Soil and Tillage Research*, vol. 154, pp. 44–52, 2015, doi: 10.1016/j.still.2015.06.011.
- [41] S. M. K. Alam and M.A. Matin, “Impact of tillage on root growth and yield of rice in silt loam soil,” *Journal of Biological Sciences*, vol. 2, no. 8, pp. 548–550, 2002, doi: 10.3923/jbs.2002.548.550.
- [42] A. Dobermann, H. U. Neue, and P. Goovaerts, “Scale-dependent correlations among soil properties in two tropical lowland rice fields,” *Soil Science Society of America Journal*, vol. 61, no. 5, pp. 1483–1496, 1997, doi: 10.2136/sssaj1997.03615995006100050028x.
- [43] B. L. Jian, Y. S. Guo, C. H. Hu, L. W. Wu, and H. T. Yau, “Prediction of spindle thermal deformation and displacement using back propagation neural network,” *Sensors and Materials*, vol. 32, no. 1, pp. 431–445, 2020, doi: 10.18494/SAM.2020.2606.
- [44] G. Asadollahfardi, “Artificial neural network,” in *Water Quality Management*, Springer, 2015, pp. 77–91, doi: 10.1007/978-3-662-44725-3\_5.
- [45] T. T. X. Phuong *et al.*, “Situation of rice production and treatment straw after harvest in Thua Thien Hue Province (in Vietnam),” *Tạp chí Khoa học và công nghệ nông nghiệp Trường Đại học Nông Lâm Huế*, vol. 5, no. 3, pp. 2720–2726, Nov. 2021, doi: 10.46826/huaf-jasat.v5n3y2021.857.
- [46] M. S. M. Amin, W. Aimrun, S. M. Eltaib, and C. S. Chan, “Spatial soil variability mapping using electrical conductivity sensor for precision farming of rice,” *International Journal of Engineering and Technology*, vol. 1, no. 1, pp. 47–57, 2004.

## BIOGRAPHIES OF AUTHORS






**The-Anh Ho**    is a Ph.D. student in control and automation engineering at Can Tho University, he received a bachelor's degree in Mechatronics from Can Tho University in 2009, a master's degree in automation from Vietnam National University Ho Chi Minh City in 2015. Since 2011, he has been working at Can Tho University of Technology and Technology. Currently, he is a lecturer in automation in the automation department. He has upgraded some supervisory control and data acquisition systems for factories in Can Tho City. His research interests are automation in industry, energy saving, and geophysics in agriculture. He can be contacted at email: htanh@ctu.edu.vn.






**Van-Huu Bui**    received a master's degree from the Graduate School for International Development and Cooperation, Hiroshima University. He currently is a lecturer at the Faculty of Mechanical Engineering, at Can Tho University. His research interest includes automotive mechanic, manufacturing engineering, control engineering and automation, high-tech agriculture, and traffic planning. He can be contacted at email: bvhuu@ctu.edu.vn.






**Van-Khanh Nguyen**    received his master's degree from Ho Chi Minh University of Technology, Vietnam, in 2014 and his doctor of engineering degree from Tokyo University of Marine Science and Technology, Japan, in 2020. Since 2007, he has been a lecturer at the Faculty of Automation Technology, College of Engineering, Can Tho University. Currently, he is the head of PLC Technology and Industrial IoT Lab. His research interests concentrate on embedded systems and AIoT and IoT-based applications in environmental and agricultural control, electrocardiogram (ECG) real-time classification, and anomaly detection. He can be contacted at email: vankhanh@ctu.edu.vn.



**Dinh-Tu Nguyen**    received his Ph.D. degree from the Department of Mechanical Engineering, National Central University, Taiwan, in 2022. He is currently a lecturer at the Faculty of Mechanical Engineering, Can Tho University of Technology, Vietnam. His current research interests include artificial intelligence, image processing, data-driven analysis in smart manufacturing, and intelligent control. He can be contacted at email: ndtu@ctu.edu.vn.



**Chi-Ngon Nguyen**    received his bachelor's and master's degrees in electronic engineering from Can Tho University and the Vietnam National University, Ho Chi Minh City University of Technology, in 1996 and 2001, respectively. The degree of Ph.D. was awarded by the University of Rostock, Germany, in 2007. Since 1996, he has worked at the Can Tho University. Currently, he is an associate professor in automation at the Department of Automation Technology and a Vice Chairman of the Board of Trustees of Can Tho University. He is also a nationally distinguished lecturer and a secretary of the National Council for Professorships in electrical-electronics and automation. His research interests are AI applications, intelligent control, medical control, pattern recognition, classifications, computer vision, and agricultural automation. He can be contacted at email: nngon@ctu.edu.vn.